

An RF ToF Based Ranging Implementation for Sensor Networks

Tufan C. Karalar, Jan Rabaey
University of California, Berkeley
{tufan,jan}@eecs.berkeley.edu

Abstract- Localization is important for self-configuring sensor networks. One of the core tasks of localization is ranging (estimating distances) to reference points. In this paper a radio signal based Time of Flight (ToF) measuring ranging system for wireless sensor networks is proposed, designed and prototyped. The prototype measurement error is within -0.5m to 2m while operating at 100Mps sampling rate and using a 50MHz signal in the 2.4GHz ISM band. The system accuracy is limited by the sampling rate and can be linearly improved with increasing rates. This RF method is more cost effective than acoustic signal based ranging schemes, as it does not require ultrasonic transducers. The system is multipath resilient and can coexist with 2.4GHz band devices such as 802.11b/g networks.

I. INTRODUCTION

Ad-hoc, self-configuring sensor networks hold promise for many monitoring and control applications, such as climate control, intrusion detection, visitor guidance, and target tracking. In these applications, it is important for each node to know its own position to tag the source of sensor data and to route packets through the network. In an ad-hoc sensor network, this position information cannot be preprogrammed in every node, so a localization system is required.

This paper presents a ranging subsystem to measure the distance between two nodes. It is designed for use in a localization system. Its prototype is, to the authors' knowledge, the first radio frequency (RF) time of flight (ToF) based ranging system prototype for sensor networks. It computes the correct range within -0.5m to 2m and the accuracy is limited by the 100Mps sampling rate. The prototype operates in the 2.4GHz ISM band and can coexist with other devices operating in this band, such as 802.11b/g networks.

The rest of the paper is organized as follows. Section II presents the motivation and previous work. Section III presents different approaches to ranging and classifies them. Section IV discusses the chosen ranging method and addresses its issues. Section V proposes the ranging system. Section VI presents the prototype and discusses its related issues. Section VII analyzes the prototype data and draws conclusions from this analysis. Also in this section, alternative analysis methods are considered and compared. Finally Section VIII concludes the article and summarizes the results.

II. MOTIVATION AND PREVIOUS WORK

In a self-configuring sensor network, most sensor nodes are deployed without any presumed position. Only a few nodes are given a priori information about their positions with respect to a coordinate system. These nodes are reference points and are typically called anchor nodes or beacon nodes[3]. The rest of the nodes calculate their positions using the location of and relationship to the anchor nodes. Thus, localization consists of two essential parts: 1) the range or angle to the anchor nodes and 2) the algorithm used to compute the location. Angle measurements usually involve antenna arrays, which are not practical for mounting on sensor nodes[1]. Ranges, however, can be measured using single antenna systems. Hence in this paper, ranges are used to relate to the reference points.

The most common position calculation algorithm is triangulation[2]. This method uses reference point positions and distances to compute the unknown position. Using overdetermined systems and optimization techniques, triangulation can tolerate range errors with up to 1m and still estimate the position with errors less than 0.5m [4]. Since 0.5m resolution is acceptable for the target sensor network the design goal for this paper is a range within $\pm 1\text{m}$

It should be noted that non-triangulation based localization techniques also exist. These apply convex optimization [5], or kernel-based learning techniques [6] to localize. However, such algorithms often require centralized computations and are not fit for distributed networks.

Although the triangulation algorithms receive considerable research attention, less effort has been spent on obtaining the range measurements on which they rely [2],[13]. Frequently employed methods are time of flight measurements using ultrasonic transducers [8], [10] as well as received signal strength (RSS) based ranging [9], [16]. Additional ToF ranging methods were proposed for use in pulse-based Ultra Wide Band (UWB) systems [11],[12]. Even less effort has gone into implementing these ranging systems as prototypes or integrated circuits [8],[9],[10].

III. CHANNEL VIEWS FOR RANGING

Different aspects of the channel can be utilized to measure ranges. Existing methods fall into three main categories that differ in the way the channel is viewed:

- Time domain view
- Frequency domain amplitude view
- Frequency domain phase view

¹ This research was supported by funding from Gigascale Systems Research Center (GSRC).

A. Time Domain View

In the time domain view; the channel is described by its channel impulse response (CIR). In the absence of multipath arrivals [22], the CIR has a single filter tap

$$h(t) = C * \delta(t - \tau_0) \quad (1)$$

where τ_0 is the line of sight (LoS) ToF and C is the signal amplitude. In the presence of multipath, transmitted signal arrives at the receiver via multiple propagation paths at different delays [23]. Therefore, additional channel taps appear in the CIR along with the LoS tap. Many ranging systems use this channel view including GPS, ultrasonic transducer based and UWB-based systems [7], [8], [11], [12].

Several factors affect the accuracy of this method. First, the resolution is proportional to the bandwidth [15]. Thus, increasing the signal bandwidth and sampling rate can improve the achievable accuracy. Additionally, the LoS tap may have a time shift if the transmitter (TX) and receiver (RX) clocks are not perfectly synchronized.

B. Frequency Domain Amplitude View

The frequency domain amplitude view considers the power attenuation due to propagation. In the absence of multipath, the received signal strength (RSS) behaves as

$$|H(\omega)| \propto 1/d^\beta \quad (2)$$

where d is the range and β is the propagation factor[22].

In presence of multipath, signal components arriving via different paths may interfere destructively [23] or constructively. Hence, the channel behaves like a filter; and the channel frequency response exhibits additional attenuation and amplification in its spectrum. Thus, the overall signal attenuation is not solely due to propagation anymore but also to the channel frequency response. Due to the dependency of the RSS on the channel frequency response, these measurements require extensive calibration steps for functionality [9],[16].

Lastly, this method has very low hardware overhead for a sensor node, as the raw RSS measurements are often already available from the data communication radio.

C. Frequency Domain Phase View

The frequency domain phase view utilizes the phase shift in the frequency response for ranging. Without multipath, this relationship is linear and can be written as:

$$\angle H(\omega) = \omega \tau_0 \quad (3)$$

However, similar to the frequency domain amplitude view, the simple relationship between phase and ToF quickly disappears with multipath. Although at least one ultrasonic system uses this view [17], its use is generally rare because of the sensitivity to multipath.

IV. ISSUES WITH THE TIME DOMAIN VIEW

This paper uses the time domain view for implementation of the ranging system. The primary reason is the resiliency of this method to multipath effects. Since most sensor node applications require indoor deployment, multipath effects are expected to be common[22]. This section addresses issues with the

bandwidth, signal type and synchronization for the time domain view.

A. Fundamental Limits

The Cramer Rao Lower Bound on the ToF estimate variance ($Var(ToF)$) has been derived for UWB radar systems and is known to be:

$$Var(ToF) = \frac{1}{SNR} \left(1 + \frac{1}{SNR} \right) \frac{1}{\omega^2} \quad (4)$$

where, SNR is the signal to noise ratio and ω is the signal bandwidth [15]. From this equation, it is clear that increasing the bandwidth improves the ToF estimate.

However when a sampled system is considered, time quantization also limits the ToF estimate accuracy. In this case, the ToF is quantized to multiples of the sampling period (T_s). Assuming the ToF quantization error is within $\pm T_s/2$, the corresponding range error due to sampling becomes $\pm 150/F_s$ (m/Msps), where F_s is the sampling rate. Hence, to keep the range error within $\pm 1m$, a bandwidth of 75MHz is needed. The minimum sampling rate is thus 150Msps. This shows that sensor network localization can be realized with less than 100MHz bandwidth and without UWB (>500MHz) signals.

B. Wideband Signals

Several types of wideband signals can be utilized in a ToF ranging system. This paper considers pulse-based wide band signals, pseudo random noise (PRN) signals, chirp signals and multi carrier wide band signals.

The first alternative uses pulse-based signaling. and requires FFT, SVD and LS algorithms for processing. [11] SVD alone is a computationally expensive operation (N^3 complexity [18]) and should thus be avoided whenever possible.

PRN and chirp-based signals are often used in GPS and radars. For ranging, they use correlation, which is less complex (N^2 complexity [18]) than SVD and LS algorithms.

Multi carrier or OFDM based, signaling requires only FFT or DFT computations [23]. Out of all, it is the least complex computation ($N \log N$ [18]). Also with this method, signals with different bandwidths and hence accuracies can be generated with same piece of hardware.

In this paper OFDM signaling is selected for implementation, because of its low computational complexity and flexibility.

C. Synchronization

To achieve ToF measurements the RX must be synchronized to the TX. i.e. the RX needs to be aware of the clock offset between the two.

i. Signals with Different Speeds

One way to achieve synchronization is using signals with different speeds, such as radio signals and acoustic signals. The faster radio signal synchronizes the RX and TX and is followed by the slower acoustic signal to measure the ToF. This is a very common form of synchronization for ranging in sensor networks [7], [8], [10]. However, these systems require highly directional, expensive and high power ultrasonic transducers. Equipping each sensor node with

such transducers would significantly increase the cost and power consumption.

ii. Two Way Time Transfer

Another method to achieve synchronization is called two-way time transfer [19]. Unsynchronized ToF measurement results include the clock offset as an additive (subtractive) term. If the same measurement were carried out in the reverse direction, then the same clock offset would appear as a subtractive (additive) term. Averaging the forward and reverse measurement results cancels the contribution of the clock offset as shown in Figure 1. Also, halving the difference of the forward and reverse ToF measurements yield the clock offset between the TX and RX. A sample realization of this method is shown in Figure 2.

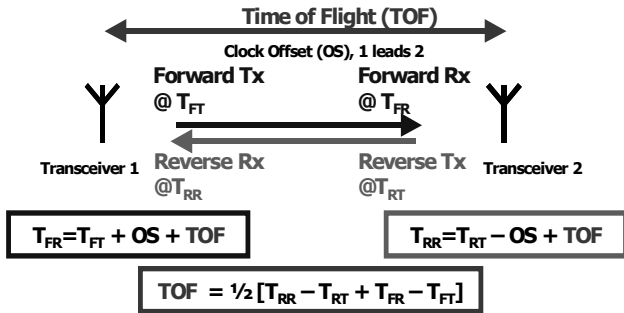


Figure 1 Illustration of the two way time transfer method for TX/RX synchronization

Two important points should be noted regarding the two-way time transfer method. First, the clock offset needs to stay constant during the forward and reverse transmissions. Typically this implies that the measurements should be carried out in rapid succession. Second, there needs to be an additional, reliable communication mechanism for exchanging transmit and receive times. For sensor networks, radios are available for data communication [20], so such exchange is readily possible.

V. RANGING SYSTEM

With the issues of the time domain view addressed, the ranging system can be designed. When an input signal X is transmitted, the received signal Y is the input filtered through the channel. To find the channel frequency response $H_{channel}$, the output frequency response can be divided by the input frequency response.

$$H_{channel}(\omega) = Y(\omega) / X(\omega) \quad (5)$$

The time of arrival can be determined by converting back to the time domain and finding the strongest channel tap in CIR. After repeating this operation for a reverse transmission, the results can be combined to calculate the ToF and clock offset. Figure 3 summarizes this process. A transmitted signal is generated by “Gen Pilot” and converted to time domain (IFFT). After DAC it is shifted up to RF. At receiver after down conversion and digitization signal is converted to frequency domain (FFT) to realize Equation 5. Finally in time domain index of the strongest CIR tap is assigned as the ToF. To meet the $\pm 1m$ error goal, the OFDM signal should have a

bandwidth of 75MHz and be sampled at 150Mps. However, as will be discussed in Section VI, the ADC and DAC in the prototype only allow up to 100Mps and hence limited the highest possible signal bandwidth to 50MHz. Therefore, this was the signal bandwidth used in the system. The OFDM signal has 128 carriers. At 100Mps, the OFDM symbol period is 1.28 μ s.

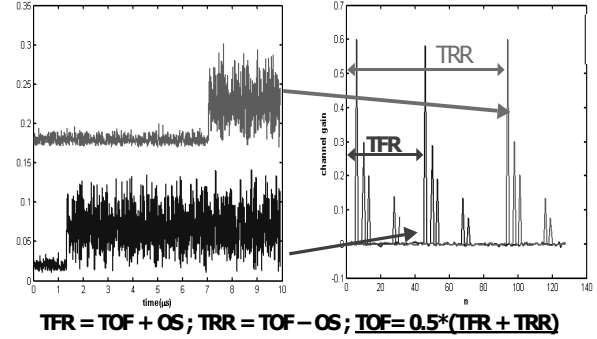


Figure 2 Simulated waveforms during forward and reverse transmissions (Left), Estimated reverse, forward and the actual channels. (Right)

The symbol period is important because the result is ambiguous if the ToF exceeds it. The maximum ranges in sensor networks are on the order of 10m-100m, so the corresponding ToFs are 30ns-0.3 μ s. Therefore, if symbol period is longer than 1 μ s, it is almost guaranteed that it will exceed the ToF. Thus, the proposed symbol period avoids any ambiguities.

The RF local oscillator offset between the RX and TX is important, as it modulates the RX output. However this modulation appears as complex gain $exp(j2\pi f_{offset})$ [23] in the CIR and does not affect the magnitude of the CIR taps. Hence the large CIR taps can be determined by observing their absolute values.

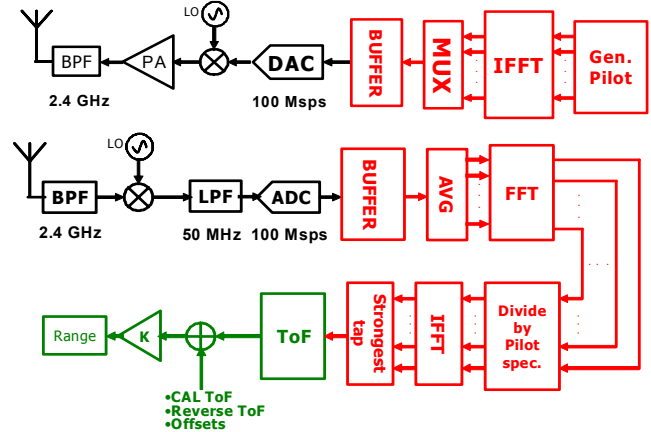


Figure 3 Block diagram of the ToF measurement ranging system. Upper chain is the TX part whereas the lower chain is the RX section.

With a 50MHz bandwidth, the system can fit in the 2.4-2.5GHz ISM band. This enables the use of existing commercial analog parts designed to work in this band for system prototyping. Additionally, the relatively high power levels allowed in this ISM band help to have enough signal strength albeit at the cost of higher interference.

VI. SYSTEM PROTOTYPE

The proposed ranging system is prototyped using FPGAs and commercial off the shelf (COTS) analog parts. The prototype consists of two parts: A baseband board and an RF board. Both the baseband and RF boards are reused from different projects [21], [24].

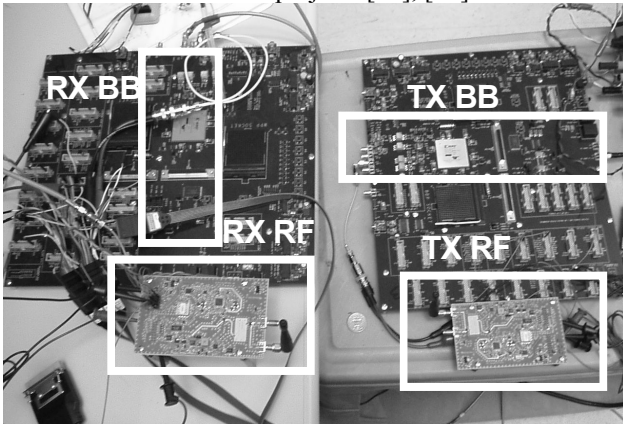


Figure 4 Photo of the prototype setup

The baseband board hosts an FPGA, an 8-bit 100Mps ADC, an 8-bit 100Mps DAC and ADC preamplifiers. The sampling rates of the ADC and DAC determine the maximum achievable signal bandwidth and accuracy.

The RF board has a frequency synthesizer used to generate the LO for the 2.4-2.5GHz frequency band. It has an RF IC that has an LNA, mixers and VGAs in the receive path. It also has an RF modulator and a power amplifier on the transmit path. A 2.4GHz bandpass filter is implemented as board trace transmission lines. The receiver mixer output filters are on-board third-order low pass discrete LC filters with 50MHz bandwidth. The prototype setup is shown in Figure 4.

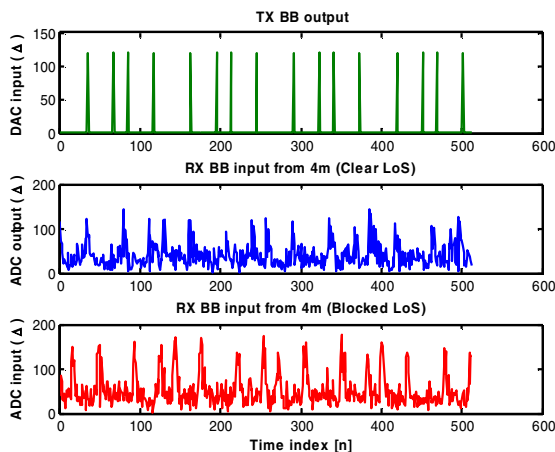


Figure 5 For a range of 4m, first plot shows transmitted signal, second plot is the received signal when LoS is clear, third is the same signal plot in presence of a LoS blocker.

Sample transmitted and received signals with this setup are shown in Figure 5. Note that, the presence of LoS blockers such as dry walls or wooden doors does not significantly attenuate the signal. Four OFDM symbol length of data are acquired per sampling window. This is equivalent to a $5.12\mu\text{s}$ sampling time window.

Before analyzing the prototype data, there are also a few practical problems that remain to be addressed.

A. Calibration

Before data analysis, the system must be calibrated to remove the delay introduced by the analog front ends (AFE) of the TX and RX. This delay is caused by channel selection filters, parasitic filters due to board traces, RF amplifiers, antenna response, etc.

To cancel AFE effects, two sets of measurement data are used. The first set is called the calibration data (CAL) and is acquired when the transmitter and receiver are right next to each other (Figure 6). The connection can be a short ($l < 30\text{cm}$) coaxial cable or can even be wireless. This calibration data and/or its relevant parameters are stored.

The second set is the data received from the transmitter, which is now at the distance to be measured. This set is called the range under measurement (RUM) data. The main difference between CAL and RUM datasets is that CAL data includes only the effects of the AFE at the transmitter and receiver, whereas the RUM data also includes the wireless channel effects (Figure 6).

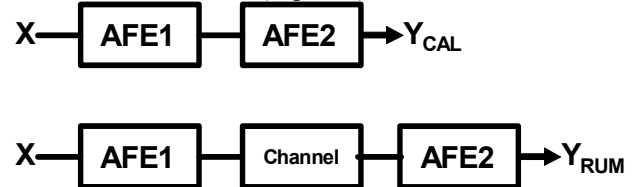


Figure 6 Block diagrams showing acquisition of calibration (CAL) and measurement (RUM) data.

B. Clock Offset

Due to physical limitations in the setup, one-way measurements are taken instead two-way time transfers. Then, an oscilloscope is used to measure the clock offset between the two nodes. The offset is defined as the delay between symbol edges, which mark the beginning of the OFDM symbols. The offset is then used to correct the ToF measurement. Due to different crystal frequencies the offset drifts during experiments while acquiring the data. Thus, to stabilize the clock offset during experiments, a single clock is fed into both nodes so the offset remains constant. In real operation, however, the forward and reverse measurements would take place within a fraction of a second and the frequency offset can be considered constant for that interval.

C. Interference Issues

Since the prototype operates in the crowded 2.4GHz band, there is interference from other devices using this band. Particularly strong interference is from an 802.11b/g WLAN access point located above the setup. Even though there are regular bursts coming from the access point (around every 20ms) its idle time is long enough to acquire the entire $5.12\mu\text{s}$ sampling window. If the acquired window coincides with a WLAN burst then the measurement is discarded and another data set is acquired. However as the WLAN gets more active, more range measurements are unusable. Aside from the WLAN network there are not any other significant interference sources detected while prototyping.

VII. RESULTS AND DATA ANALYSIS

Prototype measurements were taken as the distance between TX and RX was swept from 1.5 to 10m. To obtain ranges from this data, CAL and RUM datasets need to be combined to remove AFE effects. This can be performed in two ways:

A. Remove AFE frequency response

In the first method, the CAL data is treated as the input waveform and it is removed from the RUM data. To explain this, consider the transfer functions for Figure 6.

$$Y_{CAL} = H_{AFE1}(\omega) \times H_{AFE2}(\omega) \times X(\omega) \quad (6)$$

$$Y_{RUM} = H_{AFE1}(\omega) \times H_{channel}(\omega) \times H_{AFE2}(\omega) \times X(\omega) = H_{channel}(\omega) \times Y_{CAL} \quad (7)$$

Viewing the channel as a linear system, the CAL data can be considered as an input that is filtered by the channel to make the RUM output. Thus, dividing the RUM data by the CAL data yields the frequency response of the wireless channel and conversion back to the time domain yields the CIR. Figure 7 shows the estimated CIR for a 4m and a 6.5m test.

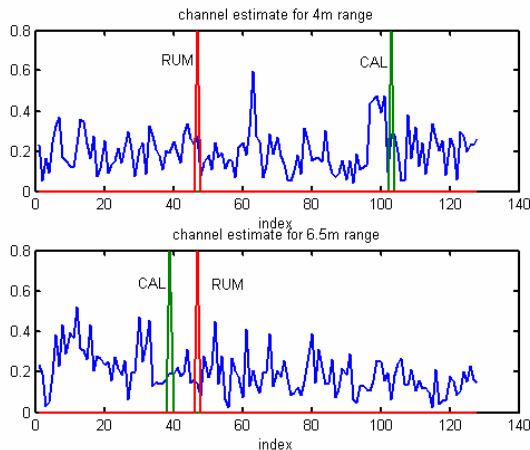


Figure 7 Estimated channel using the first method. Shown are estimated channels for 4m and 6.5m ranges respectively. Labeled spikes represent the symbol beginnings for the CAL and RUM data

Note, as can be seen in the 6.5m plot of Figure 7, the strongest CIR tap is not always clearly the dominant tap. However, if there is a clearly dominant channel tap then the ToF can be computed as:

$$ToF = n_{st} - [n_{cur_RUM} - n_{cur_CAL}] - [OS_{RUM} - OS_{CAL}] \pmod{128} \quad (8)$$

where n_{st} is the index of the strongest tap in CIR; n_{cur_RUM} , n_{cur_CAL} are the indices of the symbol beginnings for RUM, CAL data sets and OS_{RUM} , OS_{CAL} are the TX-RX clock offsets measured with an oscilloscope for RUM, CAL datasets.

B. Remove AFE delay

In the second method, the CIRs corresponding to both CAL and RUM data sets are determined separately. From these responses, the strongest channel taps are selected as the LoS taps. Figure 8 shows the estimated CIRs for CAL data and RUM data acquired when the range is 4m. Here the strongest taps are clearly dominant. Then the time of flight delay can be calculated as:

$$ToF = [n_{st_RUM} - n_{st_CAL}] - [n_{cur_RUM} - n_{cur_CAL}] - [OS_{RUM} - OS_{CAL}] \pmod{128} \quad (9)$$

where, n_{st_RUM} , n_{st_CAL} are the indices of strongest RUM, CAL taps and n_{cur_RUM} , n_{cur_CAL} , OS_{RUM} , OS_{CAL} are the same as subsection A.

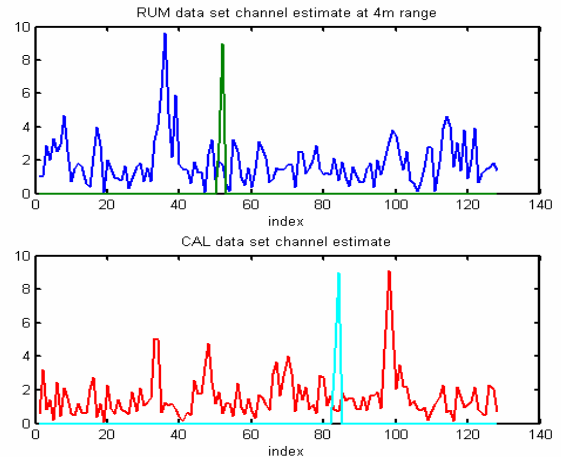


Figure 8 Estimation of RUM and CAL channels separately at range of 4m. Also shown are the symbol beginnings in each data window.

In summary, the first approach tries to remove the AFEs altogether and estimate the whole channel. In contrast, the second approach just tries to remove the extra delay due to the AFEs. In a way, the first method tries to obtain more information than is necessary, while the second method extracts only the needed data.

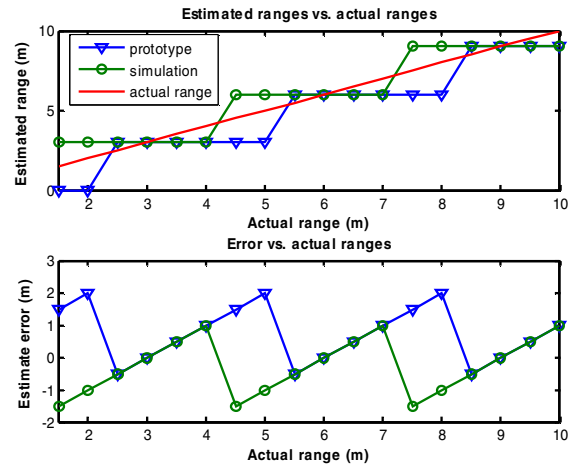


Figure 9 Distance measurement results and corresponding errors. Also shown are range estimates and associated errors from the simulations of the ranging system.

Also notable is the reduced need for data storage during delay removing method. In the first method, storage of whole calibration sequence is required and it is used each time ToF to be calculated. However in the second method, only the delay calculated from the calibration sequence needs to be stored.

C. Results

Using the ‘‘Remove AFE delay’’ analysis method, the ranges were estimated for the TX-RX distances between 1.5m and 10m. The results are plotted in Figure 9 and they

indicate that the prototype can detect ranges in 3m increments. This result is in agreement with the observation that the sampling period of 10ns corresponds to a 3m distance. This result also is in agreement with the simulated results shown in the same figure.

The bias of the estimate errors is different for the prototype and the simulations. That is, the measurements display a rounding down (flooring) quantization behavior, whereas the simulation results display a rounding quantization behavior. The discrepancy is attributed to the modeling in the simulations. The simulated channels were created as oversampled models and resampled to the ADC sampling rate of 100Msps. This resampling function causes the rounding quantization seen in the simulations.

VIII. CONCLUSION

This paper analyzed different kinds of ranging techniques and selected ToF based ranging as the implementation scheme. The shortcomings of this method are addressed by using multitone-based wideband signals and two-way time transfer. The prototype includes a calibration mechanism to account for internal delays caused by the filtering effects of the analog front ends. The result is an estimation within -0.5m to 2m that can be improved by increasing the sampling rate. This system prototype was shown to be functional despite multipath and 2.4GHz interference.

ACKNOWLEDGMENT

The authors would like to acknowledge the technical support from Fred Burghardt. Intel Corporation is acknowledged for donation of the RF boards. Also Michael A. Sheets is kindly acknowledged for his suggestions while preparing this article.

REFERENCES

- [1] J. Hightower and G. Borriello, "Location systems for ubiquitous computing," *IEEE Computer*, vol. 34, no. 8, pp. 57–66, August 2001.
- [2] K. Langendoen, N. Reijers, "Distributed Localization in Wireless Sensor Networks: A Quantitative Comparison" *Computer Networks* (Elsevier), special issue on Wireless Sensor Networks, November 2003.
- [3] C. Savarese, J. Rabaey, J. Beutel, "Locationing in distributed ad-hoc wireless sensor networks" *Int. Conf. on Acoustics, Speech, and Signal Proc. (ICASSP)*, pp 2037 – 2040, Salt Lake City, UT, May 2001
- [4] C. Savarese "Robust Positioning Algorithms for Distributed Ad-Hoc Wireless Sensor Networks," MS Thesis, University of California, Berkeley, May 2002.
- [5] L. Doherty, K. Pister, and L. El Ghaoui, "Convex Position Estimation in Wireless Sensor Networks," *IEEE Infocom*, Anchorage, AK, April 2001.
- [6] X. Nguyen, M. Jordan, B. Sinopoli. "A kernel-based learning approach to ad hoc sensor network localization." *ACM Transactions on Sensor Networks*, Vol 1(1), 2005, pp 134-152.
- [7] N. B. Priyantha, A. Chakraborty, and H. Balakrishnan, "The cricket location-support system," *ACM MobiCom* Boston, MA, 2000.
- [8] A. Savvides, H. Park, and M. Srivastava, "The Bits and Flops of the N-hop Multilateration Primitive For Node

- Localization Problems", First ACM Inter. Workshop on Sensor Networks and App., Atlanta, September, 2002.
- [9] K. Whitehouse, C. Karlof, A. Woo, F. Jiang, D. Culler. "The Effects of Ranging Noise on Multihop Localization: an Empirical Study" *International Conference on Information Processing in Sensor Networks (IPSN '05)*, Los Angeles, California. April 25-27, 2005.
- [10] D. Moore, J. Leonard, D. Rus, S. Teller, "Robust distributed network localization with noisy range measurements," *SenSys*. ACM Press, 2004, pp. 50–61.
- [11] I. Maravic, J. Kusuma, M. Vetterli, "Low-Sampling Rate UWB Channel Characterization and Synchronization", *Journal of Communications and Networks*, Volume 5, Issue. 4, December 2003, pp 319-327.
- [12] S. Gezici, Z. Tian; G.B. Giannakis, H. Kobayashi, A.F. Molisch, H.V. Poor, Z. Sahinoglu, "Localization via ultra-wideband radios: a look at positioning aspects for future sensor networks", *Signal Processing Magazine*, IEEE Volume 22, Issue 4, July 2005 pp: 70 – 84.
- [13] A.H.Sayed, A. Tarighat, N. Khajehnouri, "Network-based wireless location challenges faced in developing techniques for accurate wireless location information", *Signal Processing Magazine*, IEEE Volume 22, Issue 4, July 2005, pp: 24- 40
- [14] K. Whitehouse and D. Culler, "Calibration as parameter estimation in sensor networks," in *First ACM Int. Workshop on Wireless Sensor Networks and Application (WSNA)*, (Atlanta, GA), pp. 59–67, Sept. 2002.
- [15] H. Van Trees "Estimation Detection and Modulation Theory, Vol. 3", Wiley, New York 2001, p.299.
- [16] R. Christ, R. Lavigne, "Radio Frequency based personnel location systems", *International Carnahan conference on Security Technology*, 2000, pp141-150.
- [17] T. Kimura; S. Wadaka, K. Misu, T. Nagatsuka, T. Tajime, M. Koike, "A high resolution ultrasonic range measurement method using double frequencies and phase detection". *1995 IEEE Ultrasonics Symposium. Proceedings*.
- [18] J. Demmel, *Applied Numerical Linear Algebra*, SIAM, Philadelphia, 1997.
- [19] D. W. Hanson, "Fundamentals of Two-Way Time Transfer by Satellite", *43rd Annual Frequency Control Symposium*, 1989 pp. 174-178.
- [20] J. Rabaey et al "PicoRadio supports ad-hoc ultra-power wireless networking," *IEEE Computer*, July 2000 vol. 33, no. 7, pp. 42 – 48,.
- [21] M. J. Ammer, M. Sheets, T. Karalar, M. Kuulusa, J. Rabaey, "A Low-Energy Chip-Set for Wireless Intercom," *Proceedings of the Design Automation Conference (DAC)*, Anaheim, CA, June 2-6, 2003.
- [22] T. S. Rappaport, "Wireless Communications: Principles and Practice", 2nd ed., Pearson Education International, 2002
- [23] J. G. Proakis, "Digital communications", 4th ed., McGraw and Hill, 2001
- [24] Multi Carrier Multi Antenna research group, <http://bwrc.eecs.berkeley.edu/research/MCMA/>.